Available online at www.sciencedirect.com
ScienceDirect
Chinese Journal of Natural Medicines 2022, **20**(2): 148-154
doi: 10.1016/S1875-5364(22)60161-4
Chinese Journal of Natural Medicines

•Research article•

Dysideanones F−G and dysiherbols D−E, unusual sesquiterpene quinones with rearranged skeletons from the marine sponge *Dysidea avara*

LIU Hong-Yan [1, 2], ZHOU Mi[1], SHANG Ru-Yi[2], HONG Li-Li[2], WANG Guang-Hui[1], TIAN Wen-Jing[1], JIAO Wei-Hua[2*], CHEN Hai-Feng[1*], LIN Hou-Wen[1, 2*]

[1] *School of Pharmaceutical Sciences, Xiamen University, Xiamen 361102, China;*
[2] *Research Center for Marine Drugs, State Key Laboratory of Oncogene and Related Genes, Department of Pharmacy, Renji Hospital, Shanghai Jiao Tong University School of Medicine, Shanghai 200127, China*

Available online 20 Feb., 2022

[ABSTRACT] Four new sesquiterpene quinone meroterpenoids, dysideanones F−G (**1**−**2**) and dysiherbols D−E (**3**−**4**), were isolated from the marine sponge *Dysidea avara* collected from the South China Sea. The new structures were elucidated by extensive analysis of spectroscopic data including HR-MS and 1D and 2D NMR spectra, and their absolute configurations were assigned by single-crystal X-ray diffraction and ECD calculations. Anti-inflammatory evaluation showed that dysiherbols D−E (**3**−**4**) exhibited moderate inhibitory activity on TNF-*α*-induced NF-*κ*B activation in human HEK-293T cells with IC_{50} values of 10.2 and 8.6 μmol·L^{-1}, respectively.

[KEY WORDS] *Dysidea avara*; Sesquiterpene quinones; Marine sponge; Anti-inflammatory; Marine natural products
[CLC Number] R284.1 **[Document code]** A **[Article ID]** 2095-6975(2022)02-0148-07

Introduction

Marine sponges are regarded as the oldest invertebrate with 680 million years in the ocean. They are characterized by chemical defense to compete space and nutrition during their evolution. Secondary metabolites play multiple roles in sponge chemical defense and have become an important source for marine natural products with novel structures and various biological activities [1]. In 1974, Italian chemists discovered avarol and avarone from the Mediterranean marine sponge *Dysidea avara*, which opened a new era for sesquiterpene quinone meroterpenoids [2]. So far, nearly 300 sesquiterpene quinones and their derivatives have been found, some of which showed abundant biological activities, such as HIV-I reverse transcriptase inhibitory [2], antiinvasion [3], anti-inflammatory [4-7], cytotoxic [8-10], protein tyrosine phosphatase 1B (PTP1B) inhibitory [11-15], radical scavenging [16], antiallergic [17], antimicrobial and Na^+/K^+-ATPase inhibitory effects [18], and so on.

During our ongoing discovery on sesquiterpene quinone meroterpenoids with new structures and biological activities from the South China Sea, samples of *Dysidea avara* were collected in the waters near Xisha Islands. LC-DAD-MS chemical profiling analysis of its MeOH extract revealed the presence of several peaks with unusual UV absorptions and MS fragments. Detailed chemical investigations by chromatography led to the isolation of four new sesquiterpene quinones, namely dysideanones F (**1**) and G (**2**), dysiherbols D (**3**) and E (**4**). Herein, the detail of isolation, structure elucidation, and anti-inflammatory evaluation of the four metabolites were reported.

Results and Discussion

Dysideanone F (**1**) was isolated as colorless needles. Its molecular formula was established as $C_{21}H_{28}O$ with eight double-bond equivalents (DBE) by the protonated formula at *m*/*z* 297.2209 $[M + H]^+$ observed in the DART-HR-MS spectrum of **1**. The ^1H NMR spectrum measured in $CDCl_3$ displayed resonances for four methyls, including one doublet at

[Received on] 19-Mar.-2021
[Research funding] This work was supported by the National Key Research and Development Program of China (No. 2018YFC 0310900) and the National Natural Science Foundation of China (Nos. U1605221, 82022068, 81773866, 41906075, and 41576130).
[*Corresponding author] E-mails: weihuajiao@hotmail.com (JIAO Wei-Hua); haifeng@xmu.edu.cn (CHEN Hai-Feng); franklin67@126.com (LIN Hou-Wen)
These authors have no conflict of interest to declare.

δ_H 0.92 (d, J = 6.6 Hz, H_3-13), and three singlets at δ_H 0.72 (H_3-14), 1.05 (H_3-12), and 1.62 (H_3-11) and four aliphatic methylenes in shielding range, three aromatic protons, containing two doublets at δ_H 7.08 (d, J = 8.4 Hz, H-18), 6.64 (d, J = 7.8 Hz, H-19), and one singlet at 6.48 (H-21) as well as one olefinic proton at δ_H 5.27 (H-3) in the deshielding range. Reconciliation of the ^{13}C NMR and DEPT135 with HSQC spectra uncovered 21 carbon signals, including three sp^2 nonprotonated carbons (δ_C 133.0, 136.8 and 144.3), one oxygenated sp^2 nonprotonated carbon at δ_C 153.2, two sp^3 nonprotonated carbons (δ_H 35.5 and 38.4), seven methines (δ_C 128.4, 120.3, 115.4, 113.3, 53.0, 43.2, and 31.5), four methylenes (δ_C 47.3, 37.2, 36.1, and 27.5) and four methyls (δ_C 19.6, 17.9, 15.7, and 14.9). In the light of the above investigations of the NMR data, compound **1** was deduced as a tetracyclic structure. The 2D NMR experiments allowed for the construction of the tetracyclic scaffold of **1**. The ^{1}H-^{1}H COSY spectrum showed three groups of correlations as depicted in Fig. 1, which rendered the establishment of three subunits ***a*** (C_{10}-C_1-C_2-C_3), ***b*** (C_6-C_7-C_8-C_{13}), and ***c*** (C_{18}-C_{19}). Their linkage with the remaining non-pronated carbons was established by HMBC experiment. The HMBC correlations of the four methyls helped the connection of subunits ***a*** and ***b*** to form the bicyclic sesquiterpene substructure A/B by the linkage of C_3-C_4-C_5-C_6 and C_8-C_9-C_{10}, which was deduced by the HMBC correlations of H_3-11/C-3, C-4, and C-5, H_3-12/C-4, C-5, C-6, and C-10, H_3-13/C-7, C-8, and C-10, as well as H_3-14/C-8, C-9, C-10, and C-15 (Fig. 2). Meanwhile, the four groups of HMBC correlations indicated the methyl groups at C-4, C-5, C-8, and C-9, respectively. The presence of a benzene ring D was indicated by the subunit ***c*** (C_{18}-C_{19}) coupled

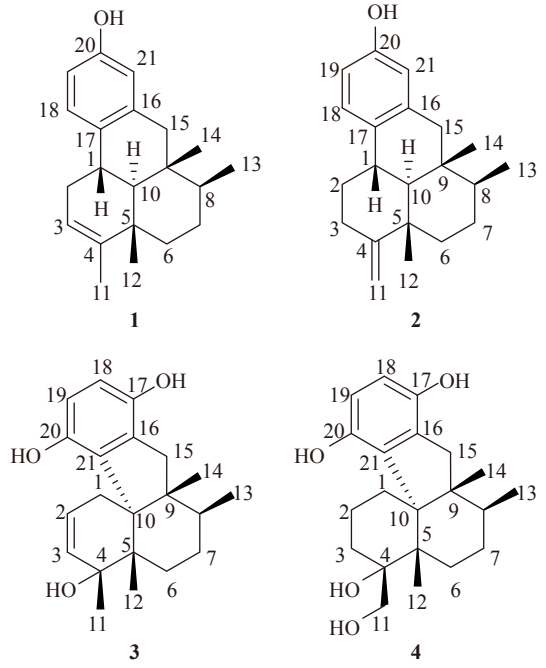

Fig. 1 Chemical structures of dysideanones F−G (1−2) and dysiherbols D−E (3−4)

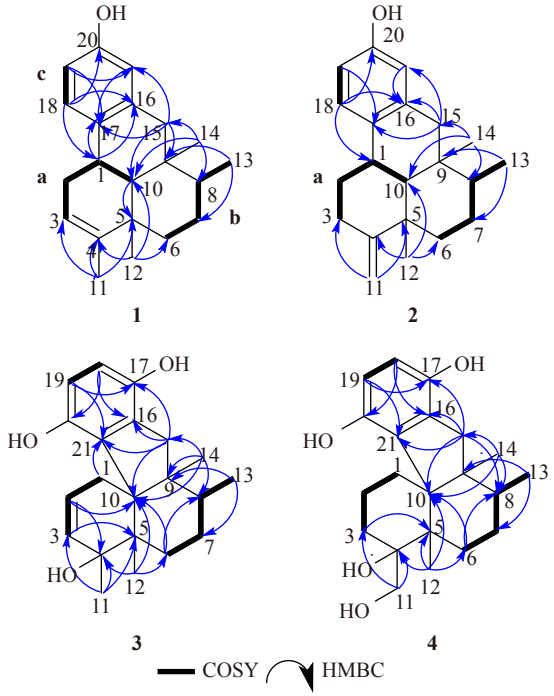

Fig. 2 Key COSY and HMBC correlations of 1−4

with HMBC correlations of H-18/ C-16 and C-20 and H-19/C-17 and C-21. The phenol hydroxy group was placed at C-20 (δC 153.2) on account of its chemical shift. (Fig. 2). The methylene H_2-15 showed common HMBC correlations with C-8, C-9, C-10, and C-14 in the bicyclic sesquiterpene part and the aromatic carbons C-16, C-17, and C-21 in the benzene ring, which connected the benzene ring D at C-15 position by C-16.

Intriguingly, the methine H-1 showed unusual HMBC correlations with aromatic carbons C-16 and C-17, indicative of a new carbon bond C_1-C_{17} to form a new six-membered ring C between the sesquiterpene part and benzene ring. This assignment was confirmed by the HMBC correlations of H-

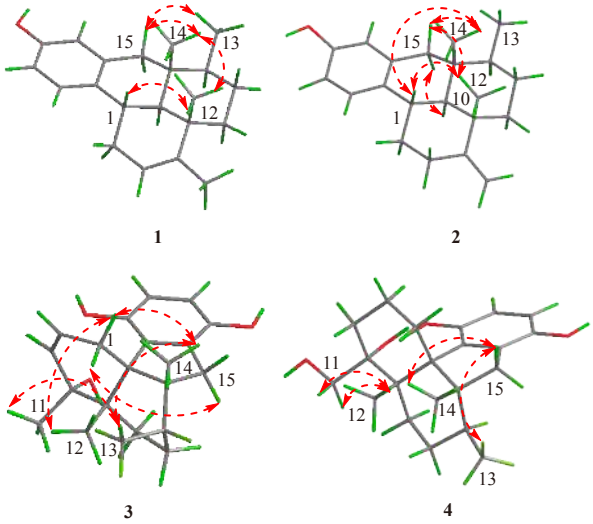

Fig. 3 Key NOESY correlations of 1−4

18/C-1. Thus the planar structure of **1** was determined as depicted.

Compound **1** possessed five chiral carbons at C-1, C-5, C-8, C-9, and C-10. Their relative configurations were assigned by *J*-based coupling constant analysis and NOESY experiment (Fig. 3). The large coupling constants between H-1 and H-10 ($^3J_{H\text{-}1,H\text{-}10}$ = 11.4 Hz) implied the axial orientation of the two protons. In the NOESY spectrum, H_3-12 showed correlations with H-1 and H_3-14, while H-15β displayed correlations with H_3-13 and H_3-14, which indicated that these protons and methyl groups were positioned on the same face. Fortunately, the crystals of **1** was obtained in the mixture of CH_2Cl_2/MeOH. Subsequent X-ray diffraction using GaKα radiation supported the proposed structure and shed light on the absolute configuration of **1** as 1*S*, 5*S*, 8*S*, 9*R*, 10*S* (Fig. 4). This assignment was further confirmed by the ECD calculations (Fig. 5).

Dysideanone G (**2**) was isolated as a white amorphous solid. Its molecular formula was established as $C_{21}H_{28}O$ by the DART-HR-MS ion observed at *m*/*z* 298.2209 $[M + H]^+$, indictive of an isomer of **1**. The high similarity of ^1H and ^{13}C NMR resonances between **1** and **2** (Table 1) suggested that they shared the same tetracyclic carbon skeleton except for the absence of a methyl (δ_H 1.62/δ_C 17.9) and an olefinic methine (δ_H 5.27/δ_C 120.3) in **1** and the presence of an exomethylene (δ_H 4.56 and 4.55/δ_C 103.3) and a methylene (δ_H 2.27, 2.55/δ_C 33.3). These differences implied that the endocyclic double bond $\Delta^{3,4}$ in **1** was swapped with an exocyclic double bond $\Delta^{4,11}$ in **2**. This proposal was confirmed by the HMBC correlations from H_3-12 to C-4, C-5, C-6, and C-10 and from H_3-11 to C-3, C-4, and C-5. The relative and absolute configurations of **2** were also determined as 1*S*, 5*S* ,8*S*, 9*R*, 10*S*, identical to those of **1**, by NOESY experiment (Fig. 3) and ECD calculations (Fig. 5).

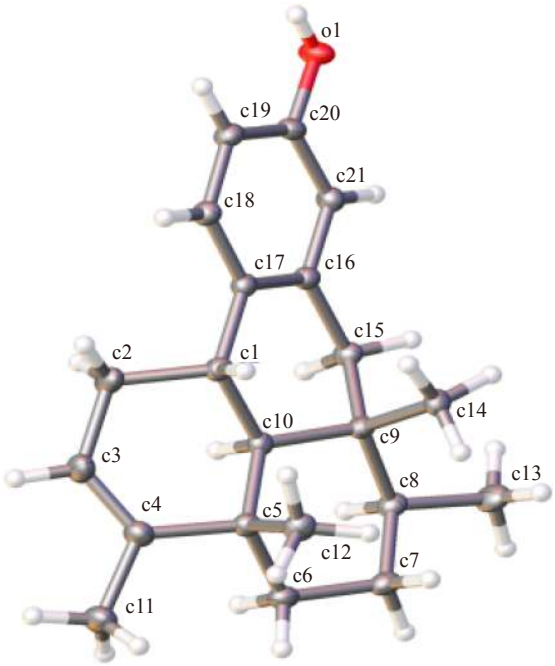

Fig. 4 ORTEP drawing of 1

Dysiherbol D (**3**) was isolated as a white amorphous sol-

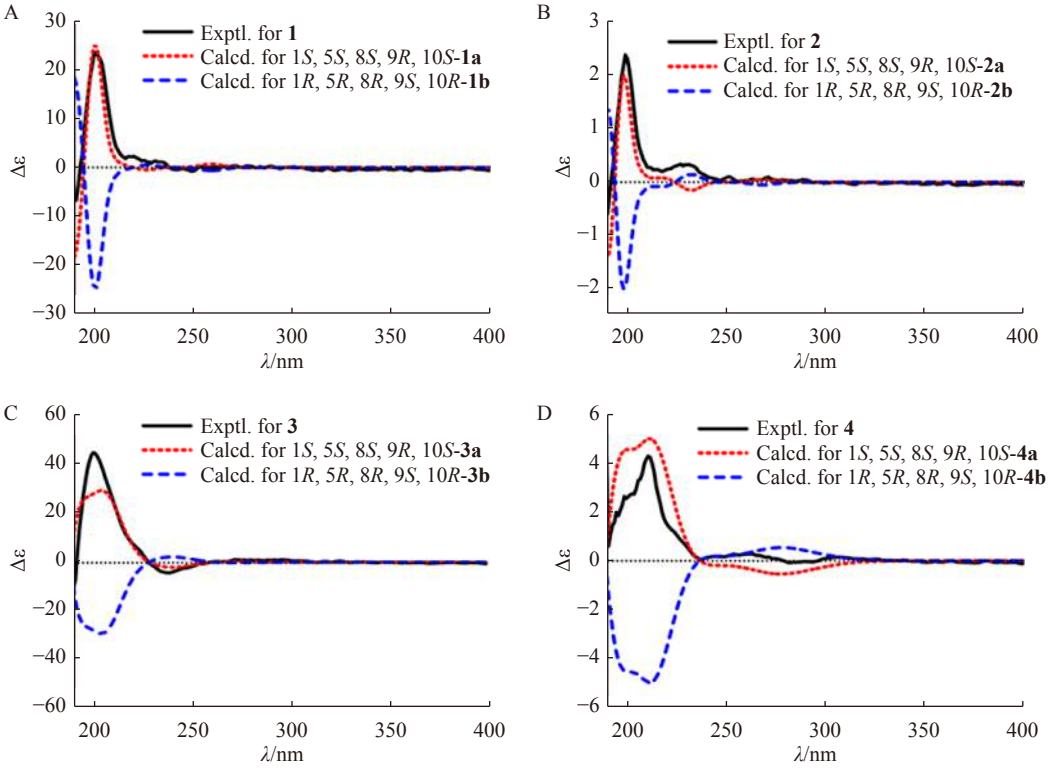

Fig. 5 Experimental ECD spectra and calculated ECD spectra of 1 (A), 2 (B), 3 (C), and 4 (D)

Table 1 ^{1}H (600 MHz, *J* in Hz) and ^{13}C (150 MHz) NMR data for **1**–**4** in $CDCl_3$

No.	1		2		3		4	
	δ_C, type	δ_H	δ_C, type	δ_H	δ_C, type	δ_H	δ_C, type	δ_H
1*α*	31.5, CH	2.94, ddd (16.2, 10.8, 5.4)	34.6, CH	2.91, ddd (11.4, 11.4, 3.0)	32.1, CH_2	2.00, dd (17.4, 4.8)	26.5, CH_2	1.87, dd, (12.6, 4.2)
1*β*						2.45, brd (18.0)		1.34, m
2*α*	36.1, CH_2	2.62, brd (13.8)	36.5, CH_2	1.28, m	129.72, CH	5.82, ddd (9.6, 5.4,1.8)	19.2, CH_2	1.59, m
2*β*		1.88, dd (13.8, 13.8)		2.45, m				
3a	120.3, CH	5.27, s	33.3, CH_2	2.54, dd (15.0, 5.4)	129.71, CH	5.37, dd (9.6, 2.4)	29.9, CH_2	2.00, dd, (14.4, 5.4)
3b				2.27, brd (13.2)				1.83, dd, (14.4, 6.0)
4	144.3, C		159.5, C		80.0, C		83.5, C	
5	38.4, C		39.6, C		36.3, C		36.9, C	
6a	37.2, CH_2	1.78, d (12.6)	37.7, CH_2	1.72, ddd (12.6, 3.6, 3.6)	29.5, CH_2	1.41, dd (9.0, 3.6)	30.5, CH_2	1.39, m
6b		1.28, m		1.61, m		1.32, m		
7	27.5, CH_2	1.47, m	27.3, CH_2	1.49, m	26.4, CH_2	1.32, m	26.3, CH_2	1.26, m
8	43.2, CH	1.28, m	43.6, CH	1.28, m	35.3, CH	1.08, m	35.3, CH	1.22, m
9	35.5, C		36.0, C		51.9, C		52.1, C	
10	53.0, CH	1.47, d (11.4)	54.9, CH	1.19, s	49.1, C		49.2, C	
11a	17.9, CH_3	1.62, s	103.3, CH_2	4.56, s	19.8, CH_3	1.35, s	65.6, CH_2	3.90, d (10.8)
11b				4.55, s				3.52, d (10.8)
12	19.6, CH_3	1.05, s	20.7, CH_3	1.12, s	18.2, CH_3	1.11, s	18.4, CH_3	1.24, s
13	15.7, CH_3	0.92, d (6.6)	15.9, CH_3	0.93, d (6.8)	17.8, CH_3	0.82, d (6.8)	17.7, CH_3	0.82, d, (6.6)
14	14.9, CH_3	0.72, s	14.6, CH_3	0.75, s	15.9, CH_3	1.13, s	14.9, CH_3	1.08, s
15*α*	47.3, CH_2	2.38, d (18.0)	47.6, CH_2	2.39, d (15.6)	39.5, CH_2	2.59, d, (15.2)	39.3, CH_2	2.56, s
15*β*		2.58, d (15.6)		2.58, d (15.6)		2.63, d, (15.2)		
16	136.8, C		137.1, C		126.5, C		126.0, C	
17	133.0, C		132.1, C		146.2, C		146.0, C	
18	128.4, CH	7.08, d (8.4)	128.4, CH	7.16, d (8.4)	115.0, CH	6.52, d (9.0)	114.4, CH	6.51, d, (8.4)
19	113.3, CH	6.64, d (7.8)	113.2, CH	6.64, d (8.4)	113.3, CH	6.45, d (8,4)	111.3, CH	6.46, d, (8.4)
20	153.2, C		153.2, C		145.7, C		147.6, C	
21	115.4, CH	6.48, s	115.4, CH	6.46, s	135.7, C		132.9, C	

id. Its formula was assigned as $C_{21}H_{28}O_3$ with eight DBE by a combination of DART-MS and ^{13}C NMR spectrum. The ^{1}H NMR spectrum of **3** (Table 1) showed three methyl singlets at δ_H 1.11 (H_3-12), 1.13 (H_3-14), and 1.35 (H_3-11), one methyl doublet at δ_H 0.82 (d, *J* = 6.8, H_3-13), two mutually coupling aromatic protons at δ_H 6.52 (1H, d, *J* = 9.0 Hz, H-18) and 6.45 (1H, d, *J* = 8.4 Hz, H-19) as well as two mutually coupling olefinic protons at δ_H 5.37 (1H, dd, *J* = 9.6, 2.4 Hz, H-3) and 5.82 (1H, ddd, *J* = 9.6, 5.4, 1.8 Hz, H-2). The ^{13}C NMR spectrum combined with HSQC spectrum exhibited 21 carbons, consisting of four aromatic nonprotonated carbons at δ_C 126.5, 135.7, two oxygenated at δ_C 145.7 and 146.2, two aromatic methines at δ_C 115.0 and 113.3, two olefinic methines at δ_C 129.71 and 129.72, four aliphatic nonprotonated carbons at δ_C 80.0 (oxygenated), 51.9, 49.1, and 36.3, one aliphatic methine at δ_C 35.3, four methylenes at δ_C 32.1, 29.5, 26.4, and 39.5, and four methyls at δ_C 19.9, 18.2, 17.8, and 15.8. Based on the above analysis of the NMR data, compound **3** was proposed as a tetracyclic structure. The ^{1}H-^{1}H COSY spectrum revealed the presence of three fragments ***a*** (C_1-C_2-C_3), ***b*** (C_6-C_7-C_8-C_{13}), and ***c*** (C_{18}-C_{19}) in Fig. 2. The six-membered ring A was constructed by the fragment ***a*** (C_1-C_2-C_3) coupled with HMBC correlations of H-2/C-4 and C-10, H-3/C-1 and C-5, H_3-11/C-3, C-4, and C-5. Another ring B, fused with ring A in the decalin moiety, was similarly established by the presence of fragment ***b*** (C_6-C_7-C_8-C_{13})

coupled with HMBC correlations H_3-12/C-4, C-5, C-6, and C-10, H_3-13/C-7, C-8, and C-9, H_3-14/C-8, C-9, and C-15, and H_2-6/C-5, C-7, C-8, and C-10. Additionally, the four methyl groups were positioned at C-4, C-5, C-8, and C-9, respectively. The quinol unit ring D was implied by the presence of remaining six aromatic carbons, the fragment ***c*** (C_{18}-C_{19}) as well as the HMBC correlations of H-19/C-17 and C-18 and H-20/C-16 and C-21. The quinol unit was linked to decalin moiety through the carbon bond C_{15}-C_{16}, which was verified by HMBC correlations of H_2-15/C-8, C-9, C-10, C-16, C-17, and C-21. Moreover, the methylene H_2-1 showed diagnostic HMBC cross-peaks with C-21, which resulted in the formation of an additional carbon bond C_{10}-C_{21} and a new five-membered ring C between the sesquiterpene ring B and the quinol ring D.

The relative configuration of **3** was assigned by *J*-based coupling constant analysis and NOESY correlations. The small coupling constants between H-2 and H-3 ($^3J_{H\text{-}2,\ H\text{-}3}$ =9.6 Hz) suggested that the double bond $\Delta^{2,3}$ was *Z* configuration. The *trans* fusion of the bicyclic ring A/B was assigned by the chemical shift of methyl C-12 (δ_C 18.2), which is consistent with that of dysiherbol A ($\delta_{C\text{-}12}$ 18.5) [8] and contrary to that of cycloaurenone B ($\delta_{C\text{-}12}$ 25.6) [18] This assignment was supported by the NOESY experiment of **3**. The cross-peaks of H_3-11/H_3-13, H-1β/H_3-13 and H_3-14, H_3-13/H_3-14, and H-1α/H-15α were clearly observed in NOESY spectrum, which indicated the relative configuration of **3** as 4*R**,5*S**,8*S**,9*R**,10*R**. Positive Cotton effect at 200 nm was exhibited in the experimental ECD spectrum of **3**, which is identical with that of the calculated 4*R*,5*S*,8*S*,9*R*,10*R*-**3a** enantiomer (Fig. 5). Thus, the absolute configuration of **3** was finally unveiled as depicted.

Dysiherbol E (**4**) was isolated as a white amorphous solid. Comparison of ^{1}H and ^{13}C NMR resonances with those of **3** unraveled that **4** was an analog of **3**. The main differences lay in the absence of one methyl CH_3-11 (δ_H 1.35/δ_C 19.8) and two olefinic methines CH-3 (δ_H 5.37/δ_C 129.71) and CH-2 (δ_H 5.82/δ_C 129.72) in **3** and the presence of an oxygenated methylene (δ_H 3.90, 3.52/δ_C 65.6) and two methylenes (δ_H 1.59/δ_C 19.2, δ_H 2.00, 1.83/δ_C 29.9) in **4**. These variations inferred that the methyl group CH_3-11 in **3** was oxygenated to a hydroxymethyl, and the double bond $\Delta^{2,3}$ in **3** was hydrogenated to two aliphatic methylenes in **4**, which was verified by HMBC correlations of H_2-11/C-3 and C-4, and H_2-3/C-5 combined with COSY correlations of H_2-1/H_2-2/H_2-3. The stereochemistry of **4** was determined as the same to that of **3** by detailed NOESY spectrum analysis (Fig. 3) and comparison of the experimental ECD with calculated ones (Fig. 5).

All compounds were evaluated for their inhibitory activity on TNF-α-induced NF-κB activation in human HEK-293T cells. Compounds **3** and **4** showed moderate inhibitory activity with IC_{50} values of 10.2 and 8.6 μmol·L^{-1}, respectively.

Experimental

General experimental procedures

Optical rotation values were detected on an Autopol VI (serial No. 91007, manufactured by Rudolph Research Analytical, Hackettstown, NJ, USA) with a 10 cm length cell at room temperature. UV spectra were measured in MeOH using a Persee TU-1950 UV-VIS spectrophotometer, and ECD data were obtained on a Chirascan CD spectrometer (Applied Photophysics). The NMR experiments were conducted on Bruker Avance DRX-600 MHz NMR spectrometers in $CDCl_3$ (δ_H 7.26/δ_C 77.00). High-resolution DART-MS spectra were acquired with a Thermo Fisher Scientific LTQ FT Ultra (No. D20201491). Column chromatography was carried out using silica gel (200−300 mesh, Qingdao) and ODS (15 μm, Santai Technologies, Inc.). TLC was performed on silica gel HSGF254 plates (Yantai) and visualized by anisaldehyde reagent. RP-HPLC was performed on a YMC-Pack Pro C_{18} RS column (250 mm × 10 mm, 5 μm) using a Waters 1525 binary HPLC pump with a Waters 2998 photodiode array detector.

Sponge material

Sponge specimens of *Dysidea avara* were collected in the waters near Xisha Islands in the South China Sea on April 3, 2015, and identified by Prof. LI Jin-He (Institute of Oceanology, CAS). The sponge was frozen in time and transported to laboratory for extraction. A voucher specimen (No. XD15408) was deposited at the Research Center for Marine Drugs, Renji Hospital, Shanghai Jiao Tong University School of Medicine, Shanghai, China.

Extraction and isolation

The frozen sponge (No. XD15408) (230 g, wet weight) was cut into pieces and then extracted with MeOH three times at room temperature to afford an extract (15.6 g) after solvent evaporation. The extract was partitioned between H_2O (0.25 L)and EtOAc (0.25 L × 3). The organic layer (7.5 g) was then suspended in 0.25 L 90% aqueous MeOH and partitioned against the same volume of petroleum ether three times. The 90% aqueous MeOH layer (5.4 g) was transferred to vacuum liquid chromatography on silica gel eluted with petroleum ether with increasing proportions of EtOAc and then EtOAc with increasing proportions of MeOH to give 11 fractions (Fr. DA−Fr. DK). Fr. DG (0.8 g) was separated by MPLC on ODS with a MeCN/H_2O gradient to obtain eight fractions Fr. DG1−Fr. DG8. Fr. DG3 (24.3 mg) was subjected to a reversed-phase (RP) C_{18} column by HPLC (MeCN/H_2O, 82 : 18, isocratic, 2 mL·min^{-1}) to get dysiherbol D (**3**, t_R = 21.6 min; 1.7 mg). Fr. DG4 (50.2 mg) was further purified by RP C_{18} HPLC (MeCN/H_2O, 90 : 10, isocratic, 2 mL·min^{-1}), yielding dysideanone F (**1**, t_R = 27.0 min; 3.5 mg) and dysideanone G (**2**, t_R = 34.6 min; 1.0 mg). Fr. DI (0.29 g) was subsequently fractioned over reversed-phase MPLC with linear gradient elution of MeOH/H_2O to give six fractions, Fr. DI1−Fr. DI6. Fr. DI6 (30.4 mg) was then separated with semipreparative reversed-phase HPLC (MeCN/H_2O, 48 : 52, isocratic, 2 mL·min^{-1}), obtained dysiherbol E (**4**, t_R = 34.8 min; 1.2 mg).

Identification of compounds

Dysideanone F (**1**): colorless needles; $[\alpha]_D$ + 178.55 (*c*

0.275, MeOH); UV (MeOH) λ_{max} (logε) 280 (3.05) nm; ECD (c 0.06875 mg·mL^{-1}, MeOH) λ ($\Delta\varepsilon$) 201 (+ 23.6) nm; ^{1}H (600 MHz in $CDCl_3$) and ^{13}C (150 MHz) NMR, Tables 1 and S1; DART-HR-MS m/z 297.2209 [M + H]$^{+}$ (Calcd. for $C_{21}H_{29}O$, 297.2213).

Dysideanone G (**2**): a white amorphous solid; $[\alpha]_D$ + 16.00 (c 0.100, MeOH); UV (MeOH) λ_{max} (logε) 197 (4.04), 280 (2.79) nm; ECD (c 0.05 mg·mL^{-1}, MeOH) λ ($\Delta\varepsilon$) 200 (+ 2.4) nm; ^{1}H (600 MHz in $CDCl_3$) and ^{13}C (150 MHz) NMR, Tables 1 and S2; DART-HR-MS m/z 297.2210 [M + H]$^{+}$ (Calcd. for $C_{21}H_{29}O$, 297.2213).

Dysiherbol D (**3**): a white amorphous solid; $[\alpha]_D$ + 50.20 (c 0.10, MeOH); UV (MeOH) λ_{max} (logε) 293 (3.45) nm; ECD (c 0.1 mg·mL^{-1}, MeOH) λ ($\Delta\varepsilon$) 200 (+ 45.1) nm; ^{1}H (600 MHz in $CDCl_3$) and ^{13}C (150 MHz) NMR, Tables 1 and S3.

Dysiherbol E (**4**): a white amorphous solid; $[\alpha]_D$ + 21.13 (c 0.071, MeOH); UV (MeOH) λ_{max} (logε) 202 (4.23), 294 (3.29) nm; ECD (c 0.714 mg·mL^{-1}, MeOH) λ ($\Delta\varepsilon$) 211 (+ 4.3) nm; ^{1}H (600 MHz in $CDCl_3$) and ^{13}C (150 MHz) NMR, Tables 1 and S4;

*X-ray crystallographic analysis data of **1***

The data of **1** was collected on a Bruker D8 Venture diffractometer using GaKα radiation (λ = 1.34139 Å) at 2976.43 K in the ω/2θ scan mode. Using Olex2, the structure was solved with the ShelXT program using intrinsic phasing and refined with the ShelXL refinement package using least squares minimization. Crystal Data: $C_{21}H_{28}O$, Mw = 296.43, orthorhombic, space group $P2_12_12_1$ (no.19), a = 6.7479(5) Å, b = 16.7381(11) Å, c = 30.297(2) Å, α = 90°, β = 90°, γ = 90°, V = 3421.9(4) Å^3 , Z = 8, T = 169.99 K, Dx = 1.151 mg/m^3 , F(000) = 1296.0, μ(GaKα) = 0.333 mm^{-1} , Dcalc = 1.151 g/cm^3 , 31779 reflections measured (6.846° ≤ 2θ ≤ 109.978°), 6502 unique (R_{int} = 0.0636, Rsigma =0.0442) which were used in all calculations. The final R1 was 0.0368 (I > 2σ(I)) and wR_2 was 0.0926 (all data). Flack parameter was 0.08(18). Crystallographic data for 1 was deposited at the Cambridge Crystallographic Data Center as supplementary publication (CCDD 2045948). Copies of the data can be obtained free of charge by application to the CCDD, 12 Union Road, Cambridge CB21EZ, UK. Tel: (+ 44) 1223-336-408; Fax: (+44) 1223-336-033; Email: deposit@cccdd.cam.ac.uk.

*ECD calculations of **1**−**4***

In general, conformational analysis was carried out through randomly searching in the Sybyl-X 2.0 using the MMFF94S force field with an energy cutoff of 5.0 kcal·mol^{-1} [19]. The results showed eight, eight, two, and four lowest energy conformers for **1**, **2**, **3**, and **4**, respectively. Subsequently, the conformers were re-optimized using DFT at the PBE0-D3(BJ)/def2-SVP level in MeOH using the polarizable conductor calculation model (SMD) by the GAUSSIAN 09 program [20]. The energies, oscillator strengths, and rotational strengths (velocity) of the first 30 electronic excitations were calculated using the TDDFT methodology at the PBE0-D3(BJ)/def2-TZVP level in MeOH. The ECD spectra were simulated by the overlapping Gaussian function (half the bandwidth at 1/e peak height, sigma = 0.30 for all) [21]. To get the final spectra, the simulated spectra of the conformers were averaged according to the Boltzmann distribution theory and their relative Gibbs free energy (ΔG). By comparing the experiment spectra with the calculated model molecules, the absolute configuration of the only chiral center was determined.

Luciferase activity

Luciferase activity of the four compounds was evaluated as previously described [4]. HEK-293T cells were seeded into 96-well culture plates. After 12 h, the cells were co-transfected with two luciferase reporter plasmids pGL4.32 [luc2P/NF-κB-RE/Hygro] Vector (30 ng·mL^{-1}) and pC-DNA-Renilla (10 ng·mL^{-1}) for 12 h. The NF-κB pathway was activated with TNF-α (20 ng·mL^{-1}) and the cells were treated with dysideanones F (**1**), dysideanones G (**2**), dysiherbols D (**3**), or dysiherbols D (**4**). Then, 0.5 μmol·L^{-1} TPCA (5-(4-fluorophenyl)-2-ureidothiophene-3-carboxamide) was uesd as a positive control, which is a potent, selective inhibitor of IκB kinase-2 (IKK-2) and can inhibit the production of pro-inflammatory cytokines *in vitro* and *in vivo* and NF-κB nuclear 36 localization. After 6 h, the luciferase activity was measured using luciferase assay kits (Promega, Madison, WI, USA)

Supplementary Material

Supplementray information can be acquired by e-mail to corresponding authors.

References

[1] Mehbub MF, Lei J, Franco C, *et al*. Marine sponge derived natural products between 2001 and 2010: Trends and opportunities for discovery of bioactives [J]. *Mar Drugs*, 2014, **12**(8): 4539-4577.

[2] Minale L, Riccio R, Sodano G. Avarol, a novel sesquiterpenoid hydroquinone with a rearranged drimane skeleton from the sponge *Dysidea avara* [J]. *Tetrahedron Lett*, 1974, **15**(38): 3401-3404.

[3] Diaz-Marrero AR, Austin P, Van Soest R, *et al*. Avinosol, a meroterpenoid-nucleoside conjugate with antiinvasion activity isolated from the marine sponge *Dysidea* sp. [J]. *Org Lett*, 2006, **8**(17): 3749-3752.

[4] Gui YH, Jiao WH, Zhou M, *et al*. Septosones A–C, *in vivo* anti-inflammatory meroterpenoids with rearranged carbon skeletons from the marine sponge *Dysidea septosa* [J]. *Org Lett*, 2019, **21**(3): 767-770.

[5] Jiao WH, Cheng BH, Chen GD, *et al*. Dysiarenone, a dimeric C_{21} meroterpenoid with inhibition of COX-2 expression from the marine sponge *Dysidea arenaria* [J]. *Org Lett*, 2018, **20**(10): 3092-3095.

[6] Gui YH, Liu L, Wu W, *et al*. Discovery of nitrogenous sesquiterpene quinone derivatives from sponge *Dysidea septosa* with anti-inflammatory activity *in vivo* zebrafish model [J]. *Bioorg Chem*, 2019, **94**: 103435.

[7] Jiao WH, Shi GH, Xu TT, *et al*. Dysiherbols A–C and dysideanone E, cytotoxic and NF-κB inhibitory tetracyclic meroterpenes from a *Dysidea* sp. marine sponge [J]. *J Nat Prod*, 2016, **79**(2): 406-411.

[8] Pérez-García E, Zubía Em, Ortega MJ, *et al*. Merosesquiterpenes from two sponges of the genus *Dysidea* [J]. *J Nat Prod*, 2005, **68**(5): 653-658.
[9] Jiao WH, Xu TT, Yu HB, *et al*. Dysideanones A–C, unusual sesquiterpene quinones from the South China Sea sponge *Dysidea avara* [J]. *J Nat Prod*, 2014, **77**(2): 346-350.
[10] Li J, Gu BB, Sun F, *et al*. Sesquiterpene quinones/hydroquinones from the marine sponge Spongia *pertusa* Esper [J]. *J Nat Prod*, 2017, **80**(5): 1436-1445.
[11] McNamara CE, Larsen L, Perry NB, *et al*. Anti-inflammatory sesquiterpene-quinones from the New Zealand sponge *Dysidea* cf. *cristagalli* [J]. *J Nat Prod*, 2005, **68**(9): 1431-1433.
[12] Jiao WH, Li J, Zhang MM, *et al*. Frondoplysins A and B, unprecedented terpene-alkaloid bioconjugates from *Dysidea frondosa* [J]. *Org Lett*, 2019, **21**(16): 6190-6193.
[13] Jiao WH, Huang XJ, Yang JS, *et al*. Dysidavarones A–D, new sesquiterpene quinones from the marine sponge *Dysidea avara* [J]. *Org Lett*, 2012, **14**(1): 202-205.
[14] Jiao WH, Li J, Wang D, *et al*. Cinerols, nitrogenous meroterpenoids from the marine sponge *Dysidea cinerea* [J]. *J Nat Prod*, 2019, **82**(9): 2586-2593.
[15] Abdjul DB, Yamazaki H, Takahashi O, *et al*. Sesquiterpene hydroquinones with protein tyrosine phosphatase 1B inhibitory activities from a *Dysidea* sp. marine sponge collected in Okinawa [J]. *J Nat Prod*, 2016, **79**(7): 1842-1847.
[16] Utkina NK, Denisenko VA, Krasokhin VB, Sesquiterpenoid aminoquinones from the marine sponge *Dysidea* sp. [J]. *J Nat Prod*, 2010, **73**(4): 788-791.
[17] Jiao WH, Cheng BH, Shi GH, *et al*. Dysivillosins A–D, unusual anti-allergic meroterpenoids from the marine sponge *Dysidea villosa* [J]. *Sci Rep*, 2017, **7**(1): 8947.
[18] Kim CK, Woo JK, Kim SH, *et al*. Meroterpenoids from a tropical *Dysidea* sp. sponge [J]. *J Nat Prod*, 2015, **78**(11): 2814-2821.
[19] Sybyl Software, version X 2.0 [CP]. Tripos Associates Inc., St. Louis, MO, 2013.
[20] Gaussian 09, Revision E. 01 [CP]. Gaussian Inc., Wallingford CT, 2009.
[21] Stephens PJ, Harada N. ECD cotton effect approximated by the Gaussian curve and other methods [J]. *Chirality*, 2010, **22**(2): 229-233.

Cite this article as: LIU Hong-Yan , ZHOU Mi, SHANG Ru-Yi, HONG Li-Li, WANG Guang-Hui, TIAN Wen-Jing, JIAO Wei-Hua, CHEN Hai-Feng, LIN Hou-Wen. Dysideanones F−G and dysiherbols D−E, unusual sesquiterpene quinones with rearranged skeletons from the marine sponge *Dysidea avara* [J]. *Chin J Nat Med*, 2022, **20**(2): 148-154.